DOE/PC/79661--T3

DE90 014601

Technical Progress Report No. 5

# DEVELOPMENT OF A VORTEXING COMBUSTOR (VC) FOR SPACE/WATER HEATING APPLICATIONS (COLD FLOW MODELING)

To

U.S. Department of Energy
Pittsburgh Energy Technology Center
TPO: John C. Winslow
(Phone) 412-675-6290
P.O. Box 10940
Pittsburgh, PA 15236

for

**Project No: DE-AC22-87PC79661**

by

Dr. S. Nieh, Principal Investigator
Department of Mechanical Engineering
The Catholic University of America
Washington, D.C. 20064
(Phone) 202-635-5170

August 1988

**SUMMARY**

This technical report summarizes the research work performed and the progress achieved during the period of May 1 to July 31, 1988 under contract No. DE-AC22-87PC79661.

A series of measurements of the gas flow field was conducted on the full-scale VC model. A number of influencing factors, both configurational and operational, were studied and their effects on the aerodynamic structure in the VC test chamber were delineated. Test results showed that aerodynamics favorable for the initiation of fuel ignition and char burnout can be achieved in VC chambers. Visualization tests of particle flow on the bench-scale model demonstrated that particle behaviors in the VC chamber can be controlled aerodynamically. The test results and operational experience are deemed highly valuable for VC combustor design. In the aspect of mathematical modeling, computations of the particle flow field with the newly developed statistic-trajectory model have been made based on solved gas flow field in VC processes. The interaction of gas flow field and particle flow field in terms of gas-particle slip velocity was identified. Large gas-particle slip velocities obtained in the VC chamber are highly favorable for the combustion processes.

The project has been progressing well. Future efforts on the cold flow work will be directed to further studies of gas flow field in the full-scale VC model and the measurement of particle flow in the bench-scale model. Numerical modeling of the combustion processes in VC chambers will be continued.

## TABLE OF CONTENTS

PAGE

SUMMARY....................................................ii

LIST OF TABLES AND FIGURES.................................iv

SECTION

1. AERODYNAMICS IN THE FULL-SCALE VC MODEL.....................1

    1.1 Test Facility..........................................2

    1.2 Flow Characterization..................................5

    1.3 Test Results and Discussions..........................10

2. VISUALIZATION TEST OF PARTICLE FLOW IN THE
    BENCH-SCALE VC MODEL......................................23

3. MATHEMATICAL MODELING OF PARTICLE-PHASE FLOWS..............29

    3.1 Calculation Basis.....................................29

    3.2 Results and Discussions...............................30

REFERENCES....................................................35

## LIST OF TABLES AND FIGURES

PAGE

TABLE

1. Test Conditions........................ ...............11

2. Variation Range of the Parameters tested..................11

3. Operation Conditions of the Visualization Test............25

4. Major Dimensions of the Bench-scale VC Model..............30

5. Inlet Conditions of Gas and Particle Flows................30


FIGURE

1. Schematic Diagram of the Full-scale VC
   Cold Model Test System......................................3

2. Test Chamber Assembly of the Full-scale VC Model............4

3. Configuration of the Adjustable Air Nozzle..................6

4. Configuration of the Vortex Combustor.......................9

5. Tangential and Axial Velocity Profiles in Run #5...........14

6. Tangential and Axial Velocity Profiles in Run #7...........15

7. Tangential and Axial Velocity Profiles in Run #8...........16

8. Tangential and Axial Velocity Profiles in Run #3...........18

9. Tangential and Axial Velocity Profiles in Run #4...........19

10. Tangential and Axial Velocity Profiles in Run #6...........22

11. Particle Flow Field with Evenly Distributed
    Air Injection..............................................24

12. Particle Flow Field with Uneven Distribution
    of Air Injection...........................................26

13. Effect of Center Pipe Length on the Particle
    Flow Field.................................................28

14. Axial Velocity Distributions of Gas and Particle Flows.....31

15. Distributions of Particle Tangential Velocities............32

16. Distributions of Gas-Particle Slip Velocities..............34

# SECTION 1

## AERODYNAMICS IN THE FULL-SCALE VC MODEL

Extensive studies on the aerodynamics and particle behavior in VC chambers, carried out respectively on the bench-scale and exploratory VC models, have provided detailed information with regard to gas flow characteristics and particle movement in coal/CWF-fired vortex combustors. The measurements and observations are analyzed and discussed in the Technical Progress Reports issued previously [1, 2]. The understanding of the gas-solid flow patterns and associated affecting configurational/operational parameters is considered extremely important in VC combustor design. However, it is worth pointing out that the progress so far achieved was generated from small scale test facilities rather than actual combustors. Thus, the study of scale-up characteristics of VC combustor is deemed a necessity which can correlate the lab research achievements to the design/operation of industrial-scale combustors. A 56"-high full-scale VC model of 24" diameter was therefore designed and fabricated as introduced briefly in the previous technical progress report [2]. This full-scale VC model has been so far tested for over one hundred hours during which systematic measurements of gas flow field were conducted under 9 operating conditions. This section summarizes the progress made in the gas phase test of the full-scale VC model.

## 1.1 Test Facility

The full-scale VC model was fabricated and hooked up with the air supply system in early July. The design, fabrication, and operating experience of the exploratory and bench-scale VC models contributed uniquely to the present work. Information obtained from the measurement of the aerodynamics in the bench-scale VC model and from the shake-down test of the 0.15 MMBtu/hr VC hot model was incorporated into the full-scale VC model design. The system thus developed is shown schematically in Figure 1. The system is driven by a F.D. fan via a 6" I.D. pipe which is divided into four feedlines. Each of the four lines has an air distributor to evenly supply air to the nozzle sets by means of flexible hoses. The flow rate through each nozzle set is controlled by PVC flow regulators and is measured and digitally displayed by 415 DC thermal flowmeters. Automatic compensation of temperature and pressure and digital display enable fast and accurate readings of the air flow rate. Particles are transported and injected into the test chamber pnuematically. Fine solid entraining exhaust air goes through a bag filter before being discharged into the atmosphere.

The test chamber assembly is shown in Figure 2 along with the major dimensions. The model is made of plexiglas for the convenience of visual observation of particle behaviors. The 56"- high test chamber is divided by a contraction section to simulate the upper and lower chambers of the VC hot models. This contraction section was proven, by hot model tests, to be highly

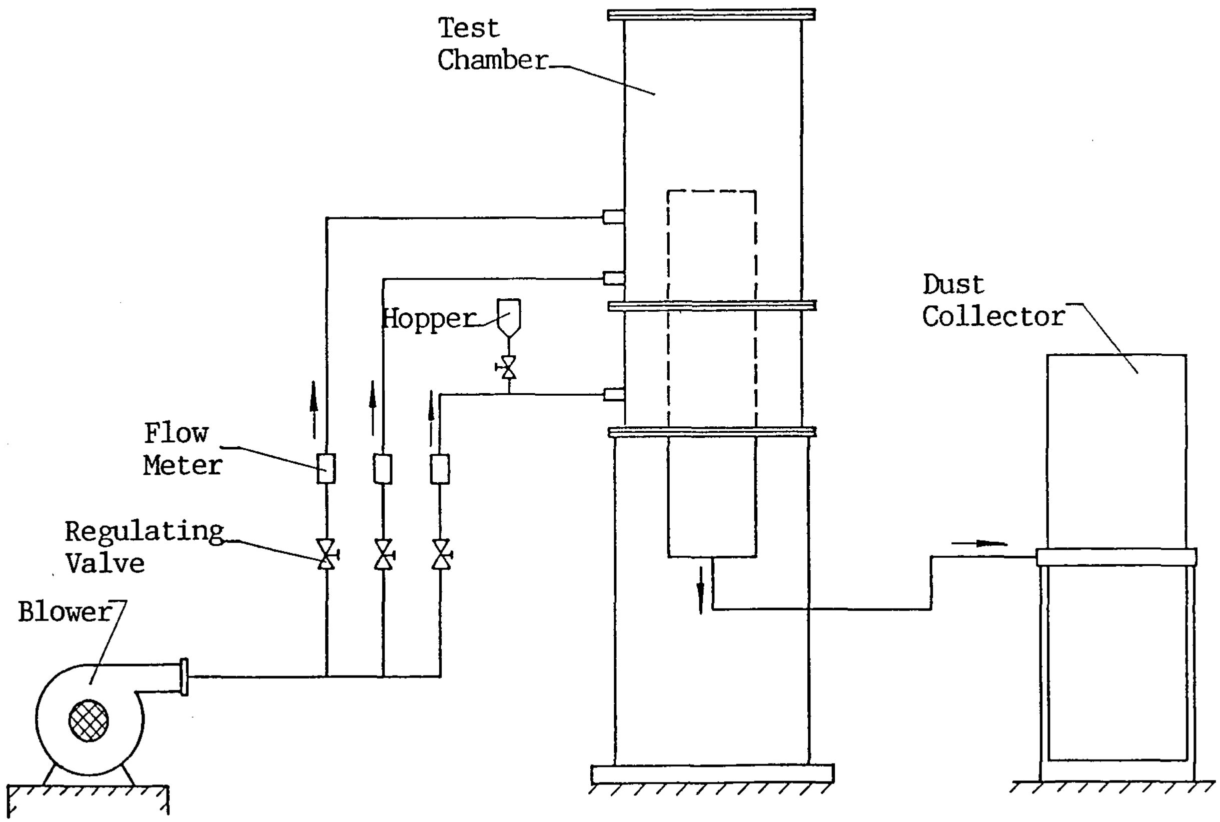


Fig. 1 Schematic Diagram of the Full-scale VC Cold Model Test System

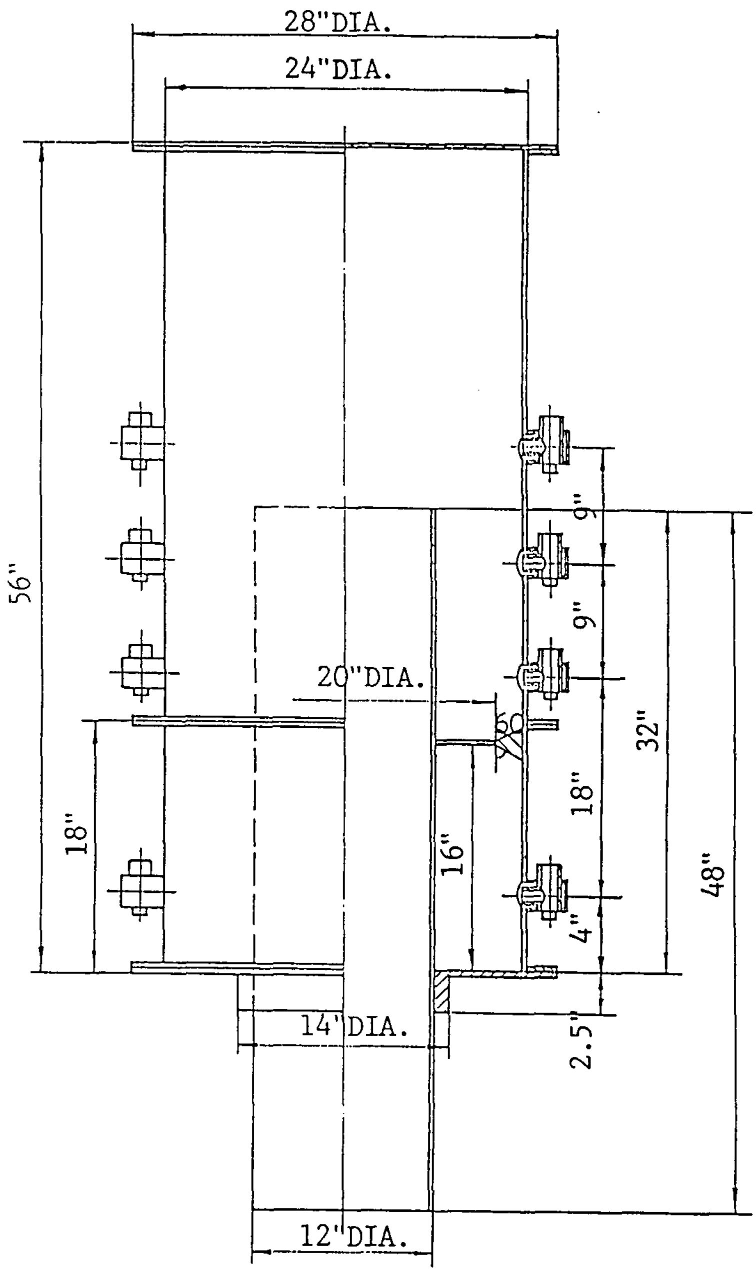


Fig. 2 Test Chamber Assembly of the Full-scale VC Model

effective in terms of fuel ignition and burnout [3]. In order to verify the effect of center pipe length on the aerodynamics and particle flow pattern, the center pipe is made adjustable along the axial direction by means of an O-ring seal on the flange mounted on the chamber bottom.

Four nozzle sets, each consisting of four nozzles, are mounted circumferentially on the test chamber at different levels. The configuration of the nozzles is shown in Figure 3. The nozzle, of rectangular cross-section, is connected to a vertically installed air pipe assembled in a panel box to form a vortex generator. The vortex generator can be turned about its axis between -30 to 15 deg. This vortex generator design enables us to change the imaginary air circle in the test chamber, hence to control the flow patterns of both gas- and particle-phase flows. Compared with the vortex generator used on the bench-scale model, the present design is much improved with regard to adjustment flexibility and simulation of real combustion processes. The lowest nozzle set is for primary air and particle feeding while the remaining three are designed for secondary air injection. Secondary air can be injected through each set of nozzles or any combination of the nozzle sets in order to study the effect of the location of secondary air injection on the gas flow pattern and particle behavior.

### 1.2 Flow Characterization

The vortex combustor presently being investigated is characterized mainly by the highly swirling flows in the

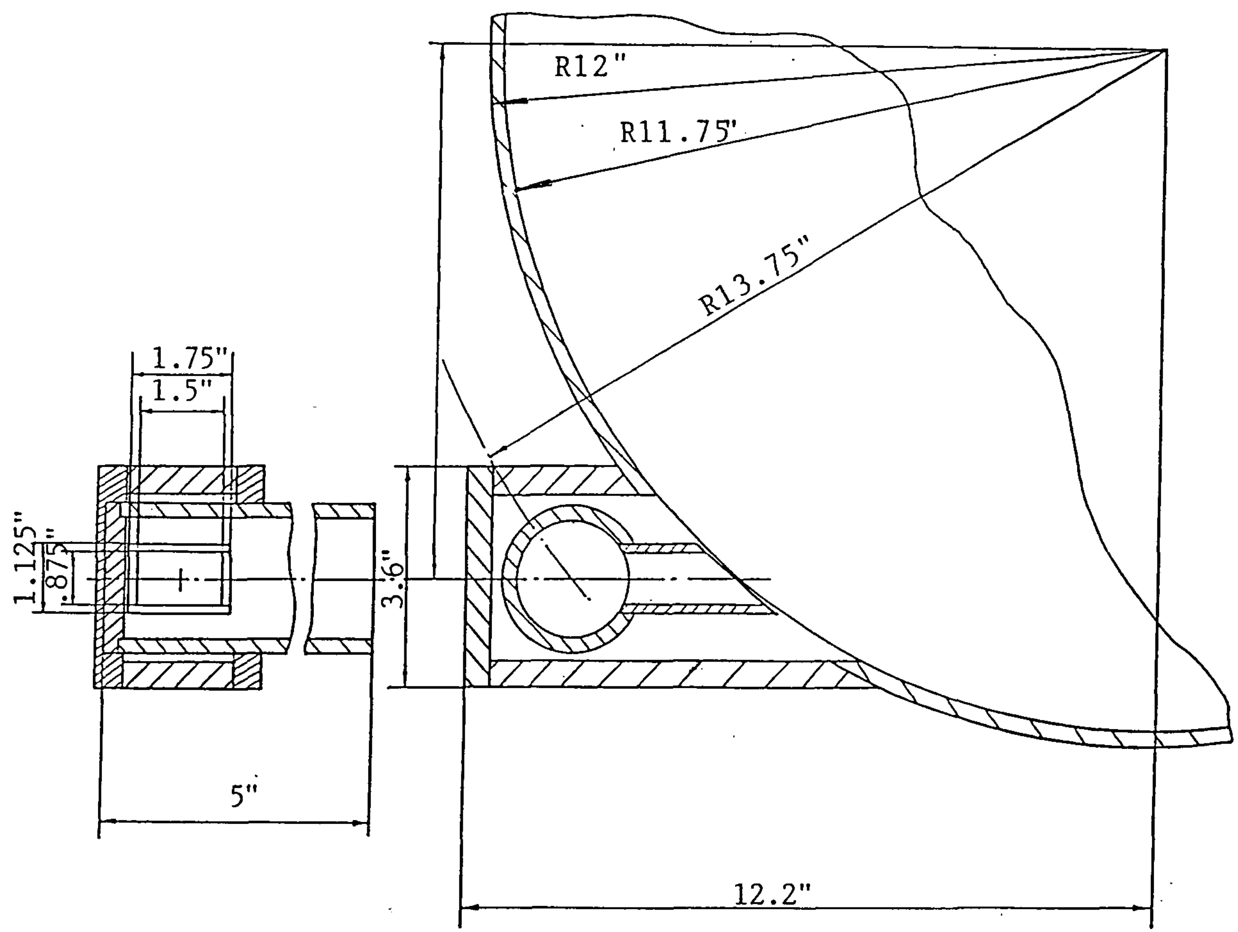


Fig. 3 Configuration of the Adjustable Air Nozzle

combustion chamber. As discussed in our previous report [1], swirl number has been employed as a suitable parameter to define the intensity of the swirling flow. Discussion of the swirl number, which takes different forms for different cases, is presented in the following paragraphs.

According to definition, the swirl number is the ratio of the axial flux of the input angular gas momentum to the product of the axial flux of the exit linear gas momentum and a characteristic radius. Simple expressions can be easily obtained from published literature for geometrically simple combustors such as swirl burners and other swirl producers. However, those expressions, generally speaking, are not appropriate for the VC due to multistage air injection, variable number of nozzles, and different injection angles. To be exact, the swirling intensity varies significantly from place to place in the VC chamber. Local swirl number was thus put forth by some investigators to describe the localized phenomenon. But the most obvious disadvantage of local swirl number is the inability to predict, on the overall, the performance of the combustor. To this end, it is clear that a proper expression of swirl number for the vortex combustor is highly desirable.

The swirl number given in the Technical Progress Report No.3

$$S = \frac{\pi \, De \, D}{4 \, At} \tag{1}$$

where

De = Combustor exit diameter
D = Diameter of the imaginary circle
At = Tangential area of the chamber

as shown in Eq.(1), is suitable for vortex generators at different levels with the same number of nozzles. the same injection angles, and the same air flow rate (which is obviously an idealized case).

Based upon the definition of swirl number and the understanding of the VC configuration and processes, an expression of swirl number for combustors with trivial configurations was derived and is shown in Eq.(2) (for detailed derivation procedures refer to [4]).

$$S = \frac{De}{4} \sum_{i=1}^{m} g_i^2 \frac{Doi}{At_i} \frac{\cos(\theta i - \alpha i)}{\cos O_i} \qquad (2)$$

where

Doi = Imaginary circle at nozzle set i
$At_i$ = Total air flow cross-section of nozzle set i
$g_i$ = Fraction of total air flow rate through nozzle set i
m = Number of nozzles in operation
$\theta_i$, $\alpha_i$ = characteristic angles (refer to Figure 4)

In the case each nozzle set has the same number of nozzles, injection angle, and air flow rate, Eq. (2) will reduce to Eq. (1). Hence, Eq. (1) is actually a simplified case of Eq. (2).

According to similarity theory, two geometrically similar

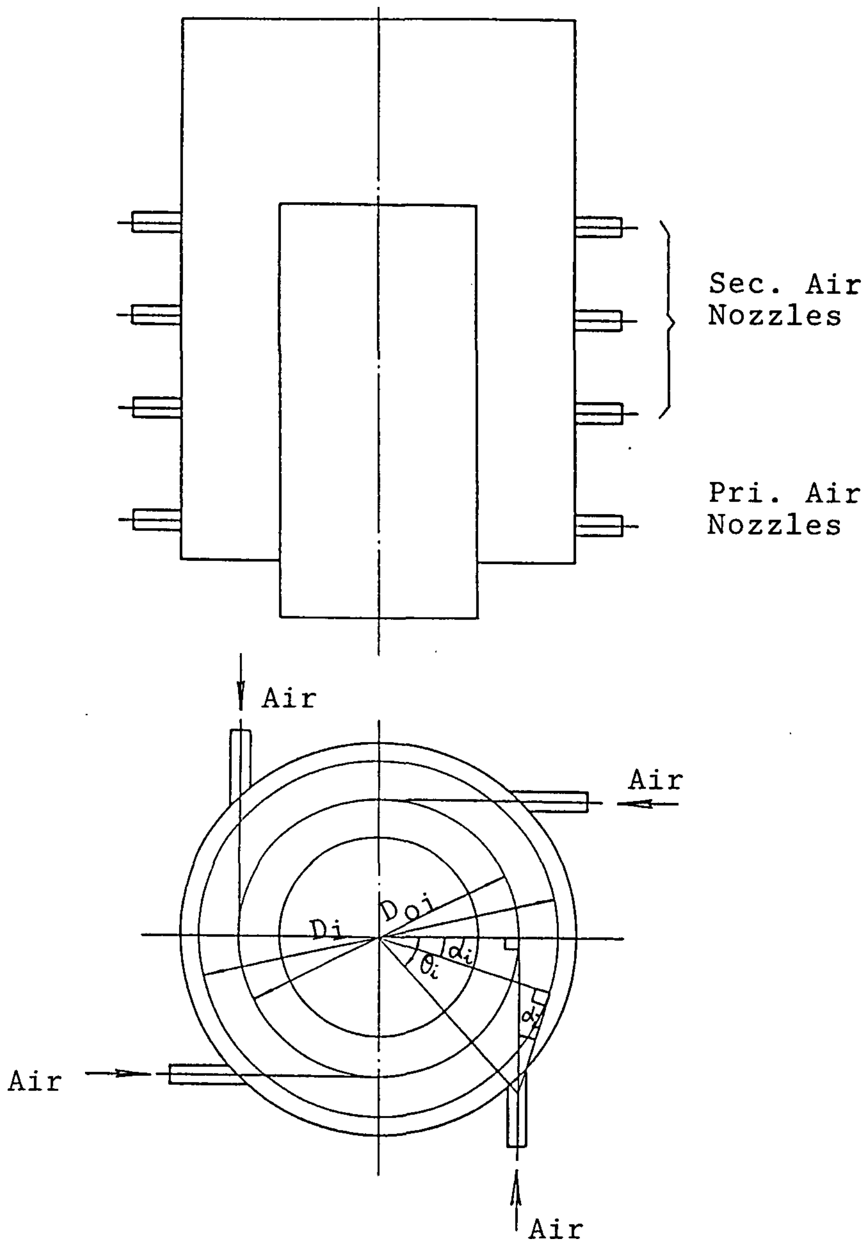


Fig. 4 Configuration of Vortex Combustor

systems should have the same swirl number to ensure similar flow structures. For combustors of simple configuration, similar flow patterns can be obtained only if they are similar geometrically. However, for combustors of complex geometry like that of the VC, to get similar flow structure requires that the two combustor should not only be similar geometrically, but also have the same air injection conditions, and hence have the same swirl number. This similarity consideration can be used for further scale-up of VC combustors.

## 1.3 Test Results and Discussions

### Conditions and Procedure

Systematic measurement of the gas flow field in the full-scale VC model has been carried out. Tangential, radial, and axial distributions of gas velocity and distributions of static pressure in the VC chamber were obtained with the 3-D directional probe presented previously [1]. Modifications of the measuring system were made to suit the model of larger scale and to ensure accurate measurement.

The following parameters were varied and studied in the test:

(i) adoption of contraction section,
(ii) center pipe length,
(iii) air injection angle,
(iv) distribution of air flow rate.

The test matrix is shown in Table 1.

Table 1. Test conditions

| No. | Q1 CFM | Q2 CFM | Q3 CFM | α1 deg | α2 deg | α3 deg | L inch | With Contraction | S - |
|---|---|---|---|---|---|---|---|---|---|
| 1 | 398 | 400 | 399 | 0 | 0 | 0 | 27.5 | No | 10.3 |
| 2 | 398 | 397 | 398 | 0 | 0 | 0 | 27.5 | Yes | 10.3 |
| 3 | 399 | 399 | 399 | 0 | 0 | 0 | 33 | Yes | 10.3 |
| 4 | 399 | 401 | 400 | 0 | 0 | 0 | 40 | Yes | 10.3 |
| 5 | 544 | 401 | 249 | 0 | 0 | 0 | 33 | Yes | 11.3 |
| 6 | 556 | 555 | 0 | 0 | 0 | / | 33 | Yes | 15.5 |
| 7 | 535 | 394 | 246 | 12 | 12 | 12 | 33 | Yes | 13.7 |
| 8 | 536 | 400 | 247 | -20 | -20 | -20 | 33 | Yes | 6.1 |
| 9 | 540 | 397 | 247 | 12 | 0 | -20 | 33 | Yes | 12.1 |

where: Q1, Q2, Q3 stand for the air flow rate through the lower, middle and upper nozzle set, respectively. L represent the center pipe length and S the swirl number. The variation range of the parameters studied are shown in Table 2.

Table 2 Range of variation of the parameters tested

| | | | |
|---|---|---|---|
| Center pipe length | L | inch | 27.5 - 40 |
| Air injection angle | α | deg | -20 - 12 |
| Swirl number | S | - | 6.1 - 15.1 |

Test Results

By examining the test results, one finds (as in the case of the bench-scale model) two distinguishable flow regions exist in the VC chamber, i.e. the annular zone between the chamber wall and center pipe and the cylindrical zone above the center pipe inlet. In the annular zone, evenly distributed tangential velocities were measured, while the axial velocity profiles are of saddle-like form, varying over the chamber height. The typical axial velocity profile has two peaks, one near the center pipe wall and the other near the chamber wall. The most interesting difference between the bench-scale model and the full-scale model is that downward (reverse) flows were detected in a wide range under most operating conditions, and in the extreme case the downward flow could even reach the lower nozzle set. This aerodynamic structure is highly significant for coal/CWF combustion. This downward (reverse) flow, which carries high temperature flue gases, can serve as a heating source for the newly injected fuel/air mixture, hence promotes initiation of fuel ignition and intensifies char combustion. In the cylindrical zone above the center pipe inlet, the tangential velocity profile is of Rankine distribution, literally

$$W r^{n} = \text{Constant} \qquad (3)$$

where n deviates a little from standard values. In the forced vortex region ($0 < r < rp$), n lies between 0 and -1 instead of being -1, whereas in free vortex region, n appears to be positive value less that 1. In other words, the tangential velocity profile in the forced vortex region is no longer a straight line but a convex curve. However, in the free vortex region, the profile exhibits a smooth curve. Change in axial velocity profile was also measured in the cylindrical zone, especially in the region near the center pipe inlet.

In order to better understand the VC aerodynamics and provide sufficient information for VC combustor design, the effects of different design/operation parameters on the gas flow pattern were primarily studied and the results are summarized in the following paragraphs.

Effects of Design/Operation Parameters

(i) Nozzle injecting angle

The change in nozzle injecting angle means to change the diameter of the imaginary circle, hence changing the swirling intensity. Runs #5, #7, #8, and #9 were designed for this purpose. The velocity profiles measured in Runs #5, #7, and #8 are depicted in Figures 5, 6, and 7, respectively. As the angle is increased from 0 deg to 12 deg, the tangential velocities increase in almost every measuring plane. In the annular space under the contraction, the tangential velocity profiles become uneven. As the angle is reduced by 20 deg, the tangential velocities reduce significantly. The average tangential velocity in Run #8 is about 3/5 of that of Run #5, and half Run #7. This is believed to be due to smaller swirl number. Significant

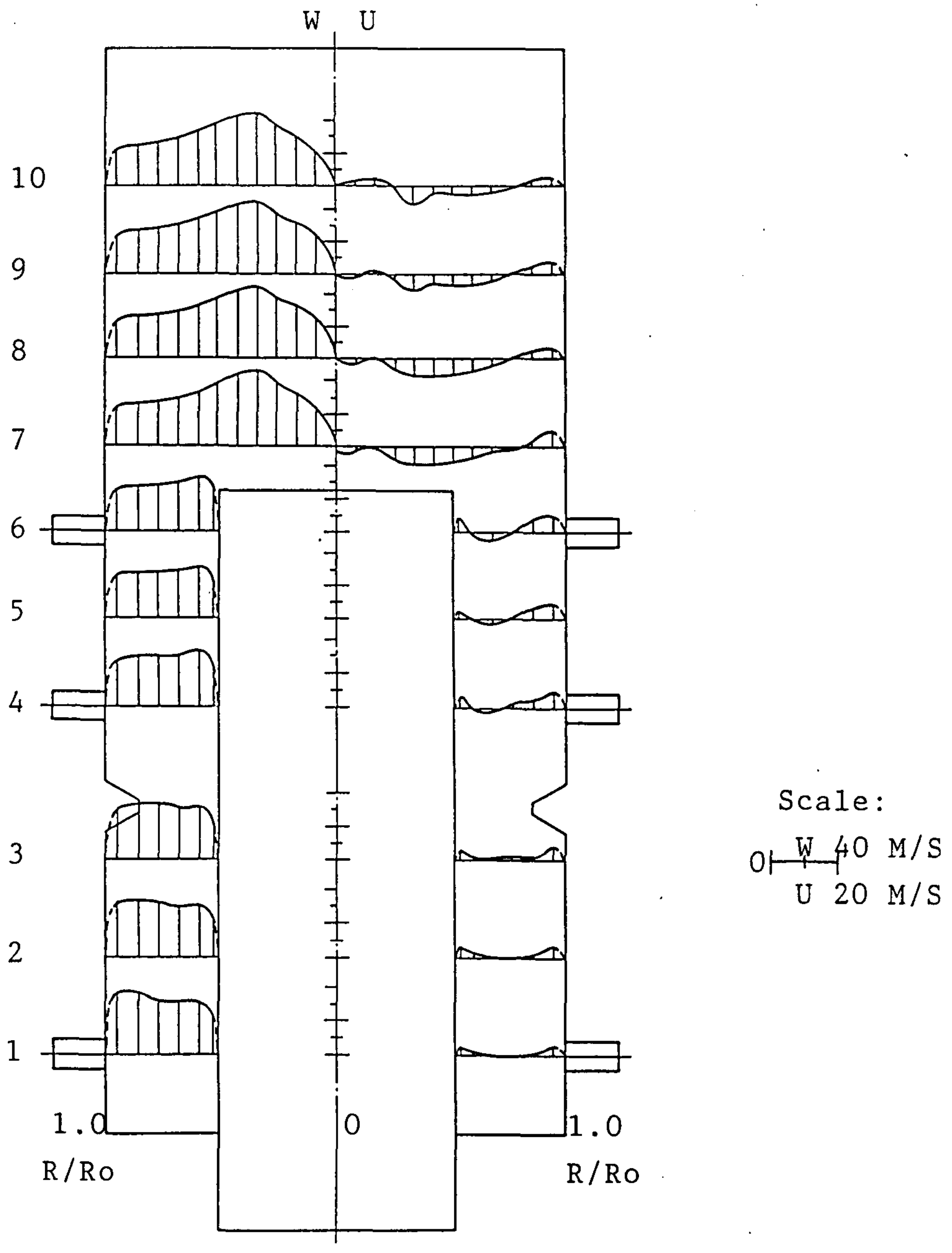


Fig. 5 Tangential and Axial Velocity Profiles in Run #5

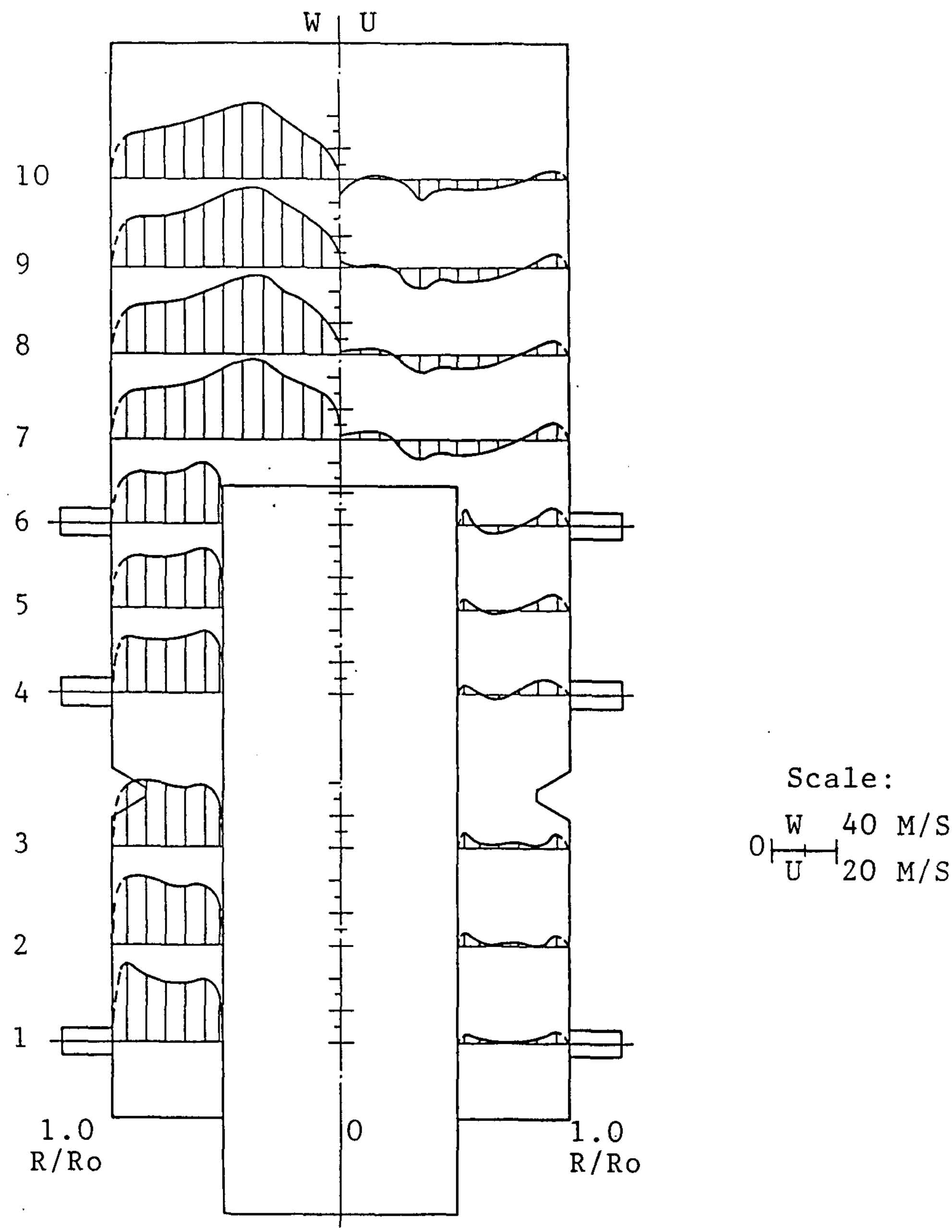


Fig. 6 Tangential and Axial Velocity Profiles in Run #7

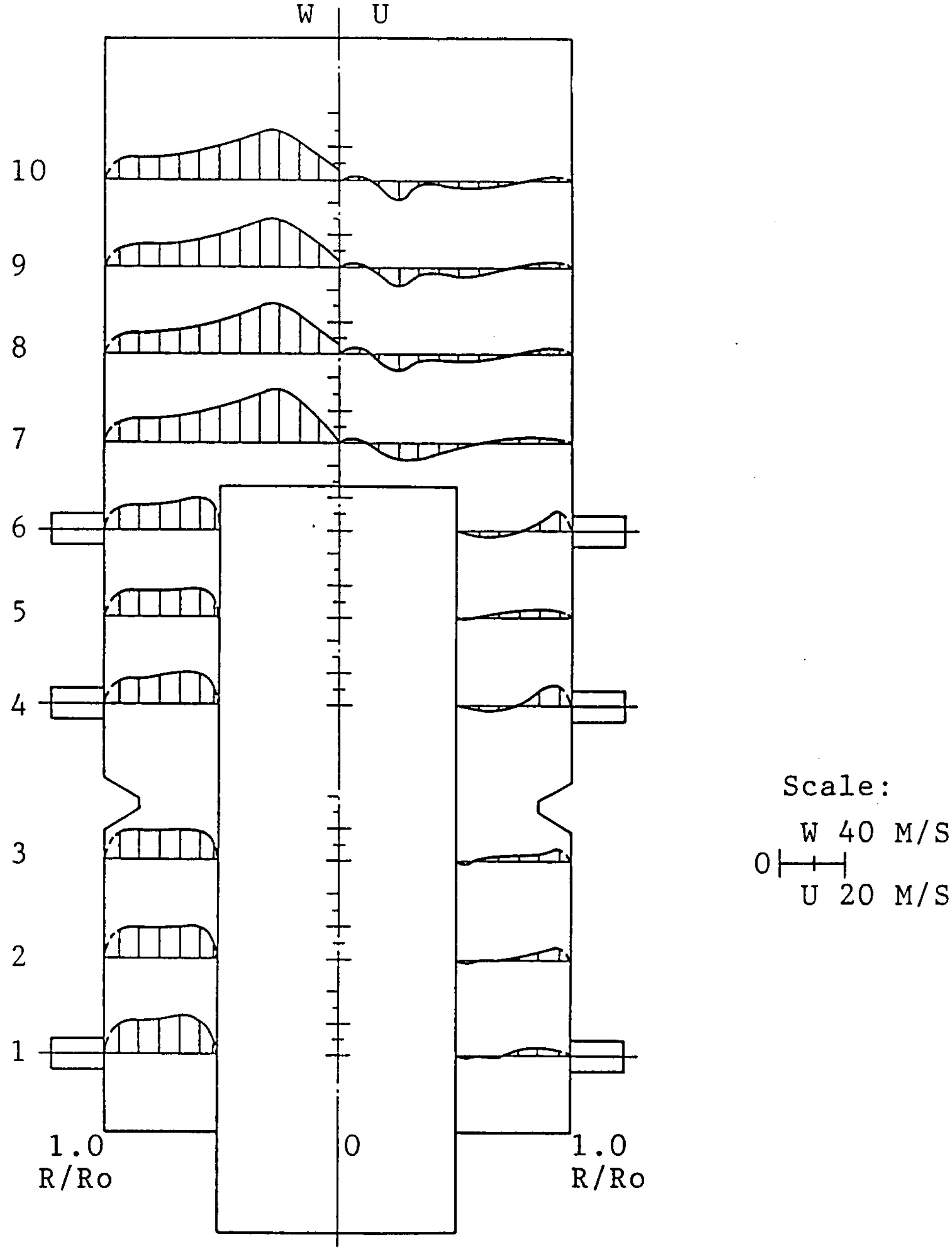


Fig. 7 Tangential and Axial Velocity Profiles in Run #8

changes of the axial velocity profile can also be perceived. The peak of the axial velocity profile near the center pipe wall disappears when the nozzle is reduced by 20 deg. In Run #8, the downward (reverse) flow was absent from most of the planes. The test results indicate that the nozzle angle is one of the key parameters that affect significantly the aerodynamics in VC chambers.

Run #9 was designed to verify the effects of focused injection of secondary air on the chamber aerodynamics. The injection angles for the lower, middle, and upper nozzle set were 12 deg, 0 deg, and -20 deg, respectively. The focused injection is supposed to produce a cone-shaped distribution of imaginary circles for better flow structure in the chamber. Measurements show that the tangential velocity profiles are not significantly affected except the unevenness below the contraction section. On the other hand, changes in axial velocity profile were observed. The peak of the saddle-like profile near the center pipe wall diminishes whilst the peak near the chamber wall increases when the model is operated in focused injection mode. The flow structure thus formed indicates that the focused injection of secondary air can help supplying oxygen to the fuel particles concentrated near the chamber wall due to the centrifugal force, thereby improving the carbon burnout of the combustor.

(ii) Center pipe length

Comparison tests with different lengths of center pipe were conducted. The velocity profiles measured are shown in Figures 8 and 9. Measurements demonstrated that with reduced center pipe

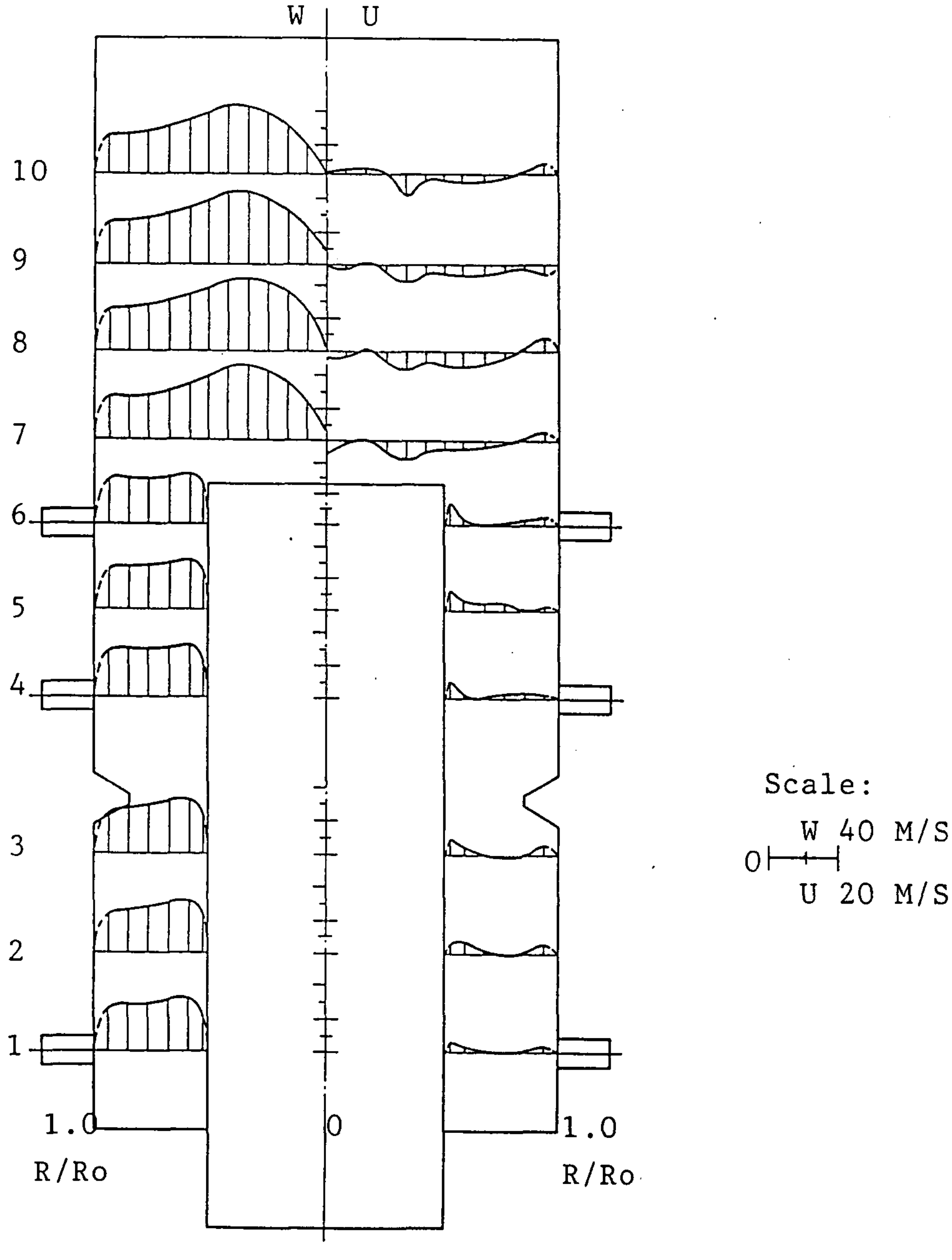


Fig. 8 Tangential and Axial Velocity Profiles in Run #3

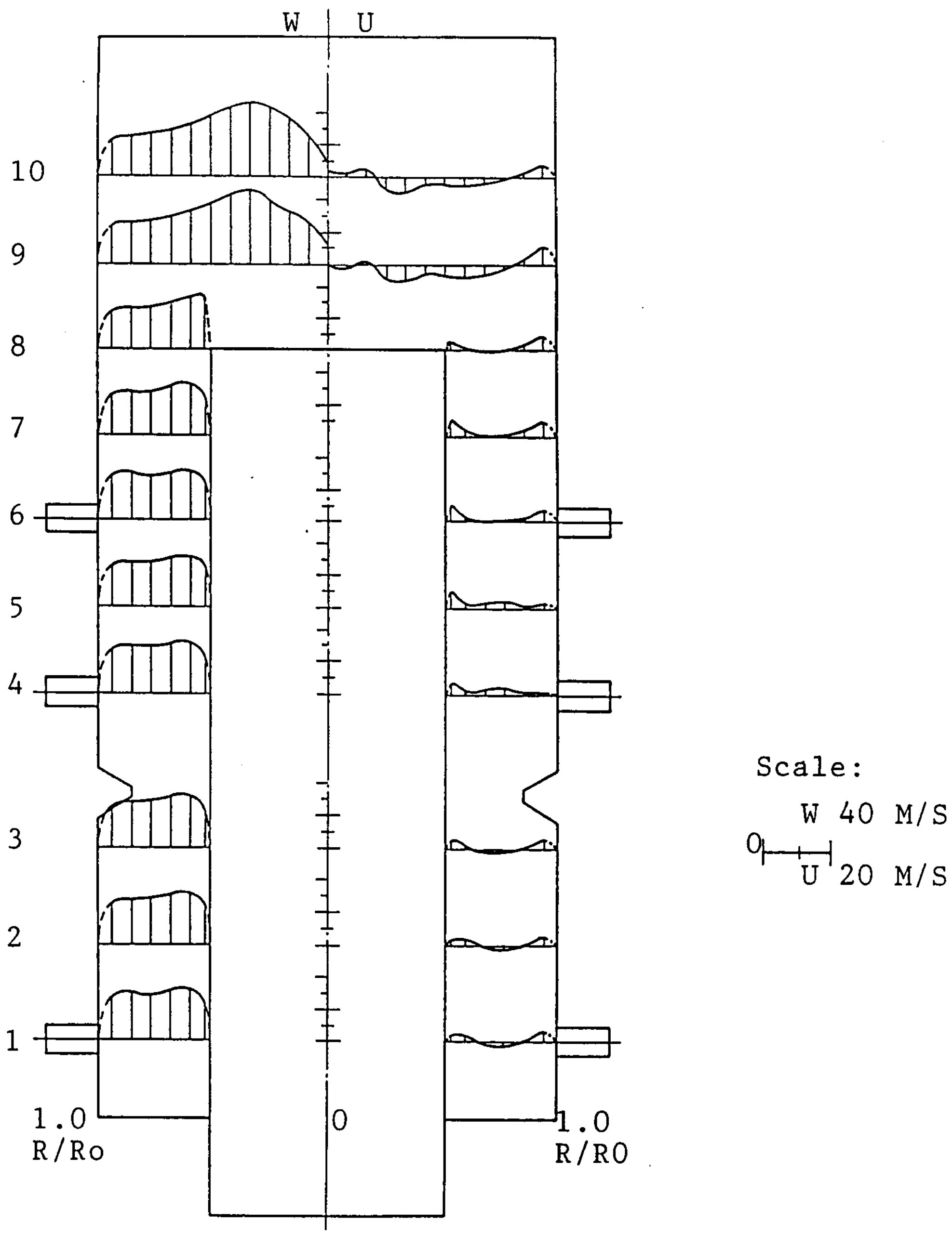


Fig. 9 Tangential and Axial Velocity Profiles in Run #4

length, the cylindrical zone, which is above the center pipe inlet and possesses the characteristics of a cyclone-type combustor, tends to be larger. This is thought to be favorable for the combustion processes in terms of mixing and reverse flow of high-temperature flue gases. However, if the center pipe length is reduced beyond a lower limit, "short circuit" of particles may occur, in other words, large amounts of particles will be carried over. This was verified by the visualization test of particle flow field and will be discussed in the next section.

(iii) Air flow ratio

The highly swirling flow in VC chambers, as discussed in 1.2, is characterized by the swirl number which depends not only on chamber configuration, but also on operation parameters. By varying the air flow ratio between the three nozzle sets (with constant total flow) different swirl numbers can be obtained. For instance, changing the distribution from Run #3, when the air was evenly distributed through the three nozzle sets, to Run #5 with uneven distribution, leads to a change of swirl number from 10.3 to 11.3. In Run #6, when air was injected through two nozzle sets, a swirl number as large as 15.5 was achieved. Figures 8 and 5 show the velocity profiles of Runs #3 and #5, respectively. Different tangential velocity profiles can be seen in the region below the contraction section. It is interesting to notice that the tangential velocities near the chamber wall become larger in Run #5. This is thought to be induced by stronger swirling flow generated by the lower nozzle set due to the larger air flow rate. No major changes in the axial velocity profile were observed in either the annular or the cylindrical zones except in the transient region between the two zones.

In Run #6 when the total air flow was evenly distributed through the middle and lower nozzle sets, higher tangential velocities were detected in almost every measuring plane (Figure 10). More important is that larger recirculation zones were formed and in some cases, the reverse flow could even reach down to the lower nozzle set. Higher axial velocities appeared near the chamber wall. This aerodynamic structure is deemed highly favorable for fuel ignition and char burnout.

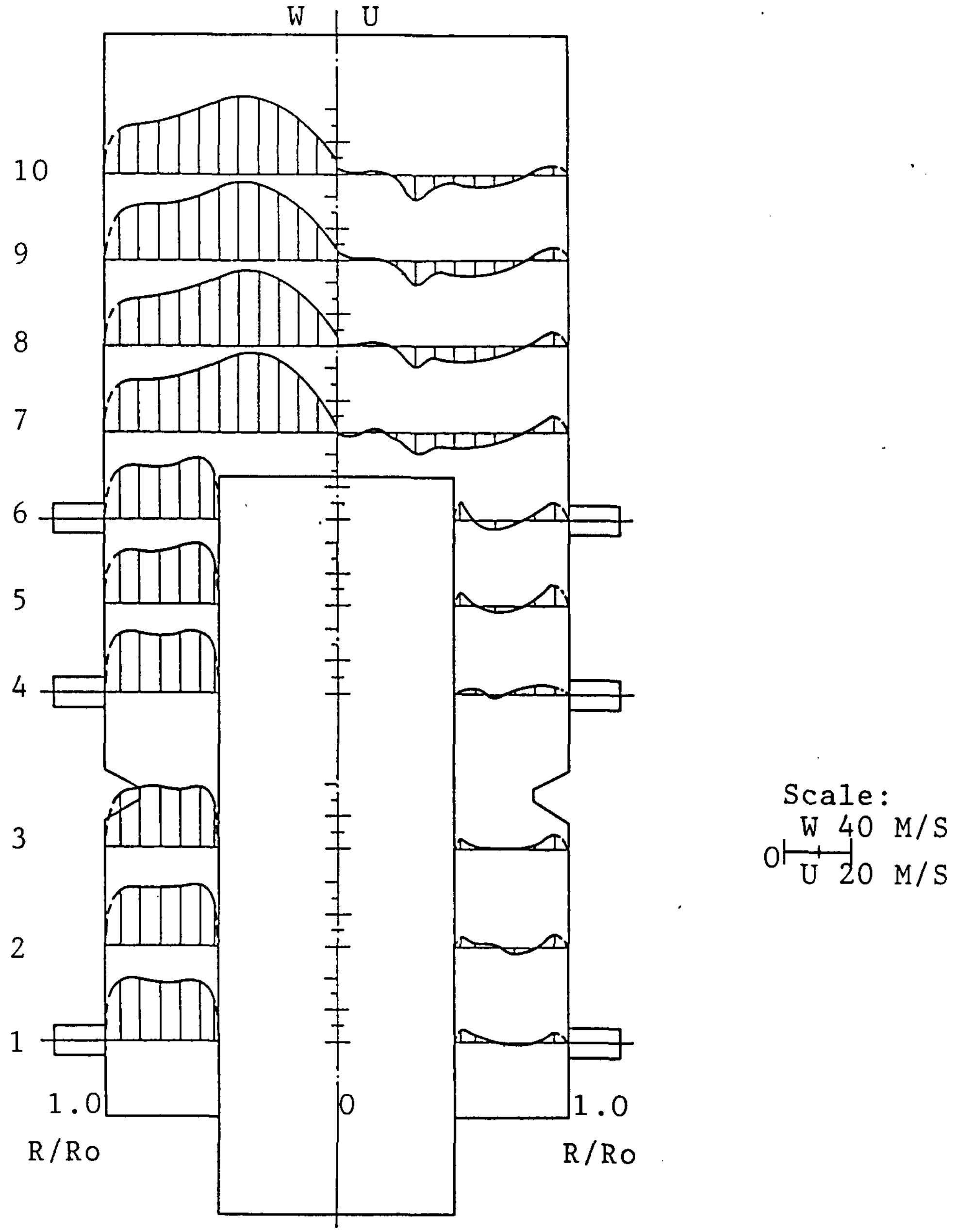


Fig. 10 Tangential and Axial Velocity Profiles in Run #6

## SECTION 2

## VISUALIZATION OF PARTICLE FLOW IN THE BENCH-SCALE VC MODEL

Studies and measurements on the VC models have so far been concentrated mainly on the aerodynamics of the vortex chamber. However, it is equally important, from combustion point of view, to study the particle flow field of the multiphase flow system as far as the initiation of fuel ignition and char burnout are concerned. TV/VCR/CAMERA were used in the present visualization studies of particle flow field to study the particle behavior and controlling parameters.

10 - 53 um colored glass beads were employed as solid material to simulate the ultrafine coal particles in VC combustors. The model was operated under focused air injection mode which appeared to be most suitable for VC combustion. The effects of different air flow rate through each nozzle set and the length of center pipe on the particle flow pattern were studied. Table 3 gives the operation conditions of the visualization test.

Fig. 11 shows the particle flow field obtained in Run #1 with evenly distributed air injection. Particles are observed all way along the chamber height with a relatively high

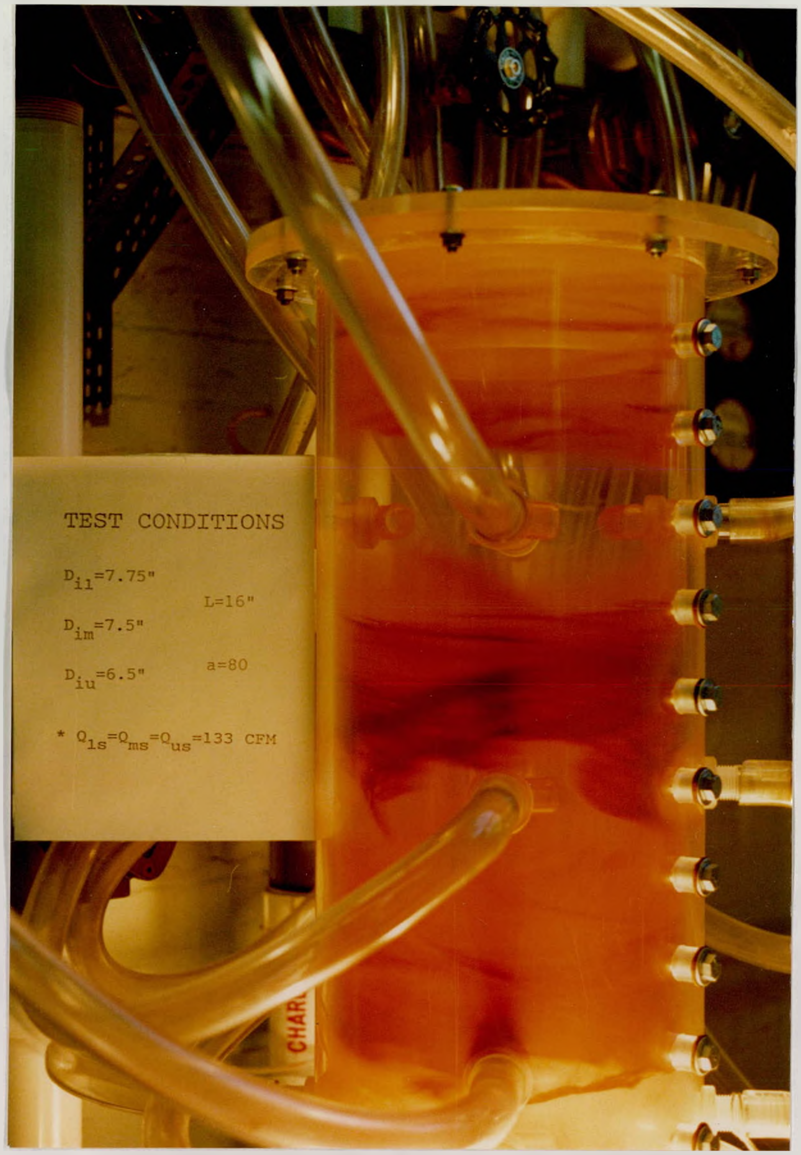


Fig.11 Particle Flow Field with Evenly Distributed Air Injection

Table 3 Operation conditions of the visualization test

| Run No. | Center pipe length (inch) | $Q_{sl}$ (CFM) | $Q_{sm}$ (CFM) | $Q_{su}$ (CFM) | $Q_p$ (CFM) |
|---|---|---|---|---|---|
| 1 | 20 | 133 | 133 | 133 | 0 |
| 2 | 16 | 133 | 133 | 133 | 0 |
| 3 | 12 | 133 | 133 | 0 | 66 |
| 4 | 16 | 133 | 133 | 0 | 0 |
| 5 | 16 | 133 | 133 | 0 | 66 |
| 6 | 16 | 133 | 0 | 133 | 0 |

concentration zone between the middle and upper nozzle set. However, particles are diluted in the region adjacent to the nozzles. The particles are carried by the air jet, which spreads upward and downward, to the zones between two nozzle sets. Particles of different sizes exhibit different behaviors due to the balance between centrifugal force, air drag force, and gravity. The greater the particle size, the longer the residence time. Figure 12 shows the particle flow field in Run #6 where no air was injected through the middle nozzle set. A particle layer can be observed along the chamber wall between the lower can upper nozzle sets with the highest particle concentration around the middle nozzle set. In the region near the upper nozzle set, dilute particle suspension forming a translucent zone around it can be seen. Similarly, with upper nozzle set shut-off, the dilute particle zone moves down to the region close to

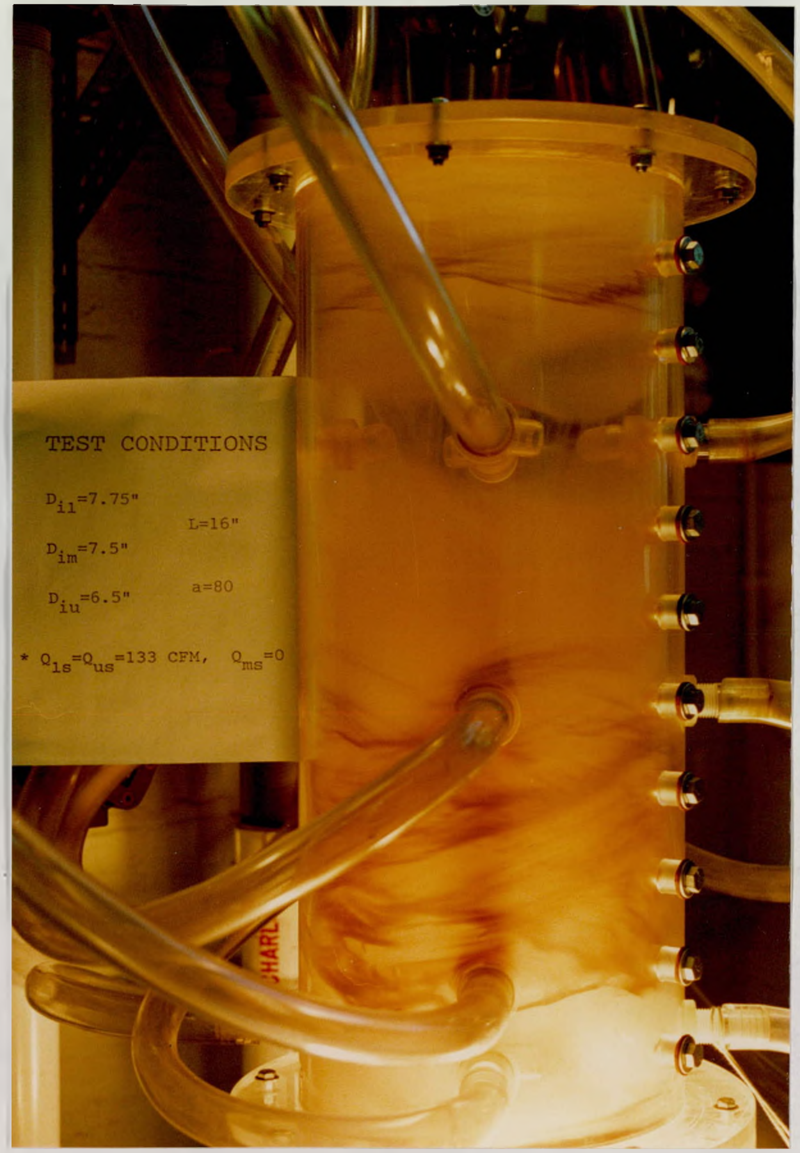


Fig.12 Particle Flow Field with Uneven Distribution of Air Injection

the middle nozzle set.

Different particle density distributions were obtained, as depicted in Fig. 13, when the center pipe length was increased from 16" to 20" while the air flow rate through each of the three nozzle sets was constant. In this case, a large number of particles are concentrated in the region above the upper nozzle set. Tests also showed that almost no particles were found in this region while the center pipe length was reduced to 12" and the particle residence time was greatly shortened which we call "short-circuit phenomenon". The "short-circuit phenomenon" will significantly affect the carbon burn-off efficiency and the effective use of sulfur sorbent. On the other hand, measurements of the aerodynamics showed that, with properly reduced center pipe length, highly turbulent vortex flow with wide range of gas recirculation can be achieved which is favorable for fuel ignition and char burn-out. More work obviously has to be done to establish criteria for center pipe design.

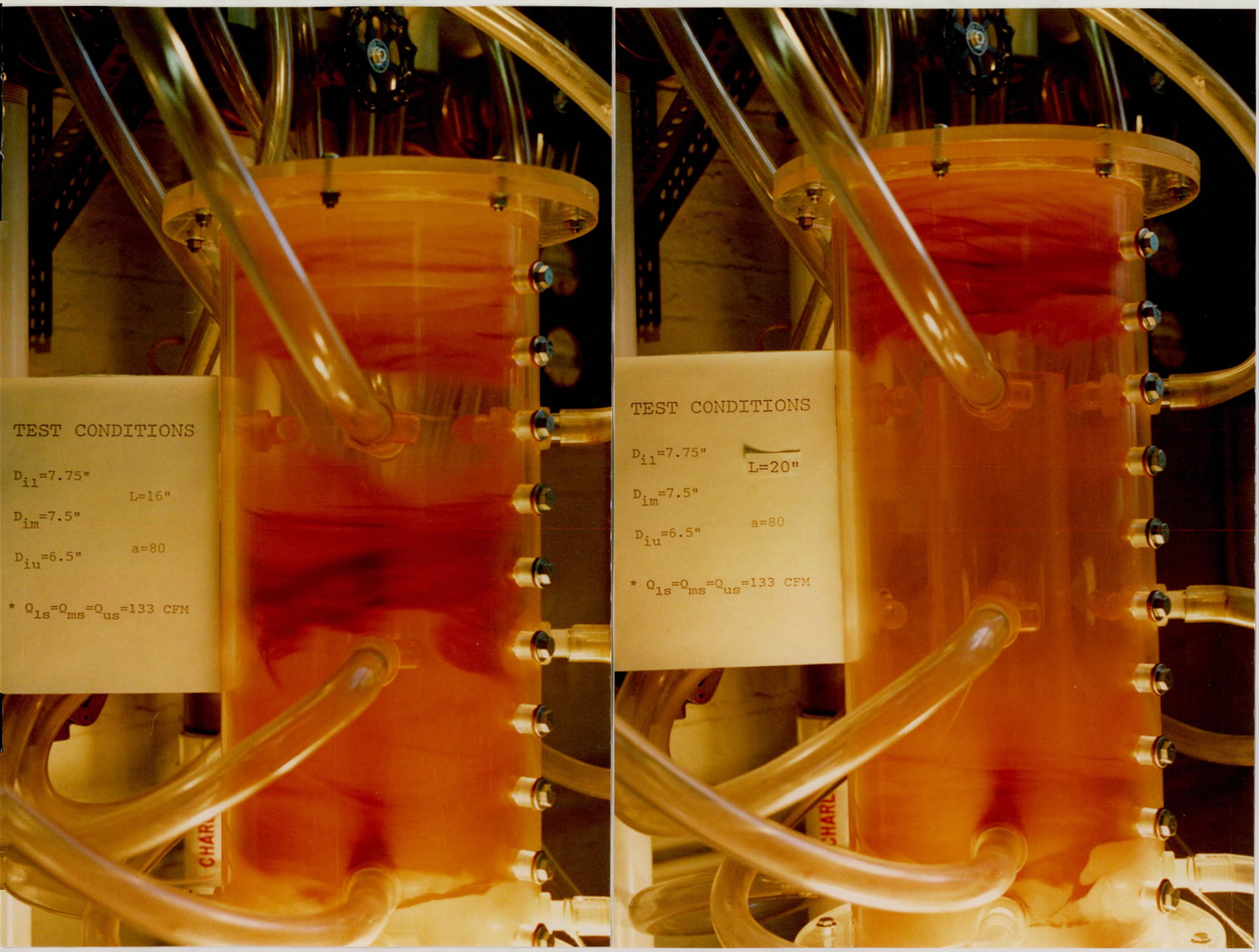


Fig.13 Effect of Center Pipe Length on the Particle Flow Field

SECTION 3

# MATHEMATICAL MODELING OF PARTICLE-PHASE FLOWS

The progress in the modeling of particle flow has led to the development of a statistical-trajectory model which was introduced briefly in the previous report [2]. A number of runs of the computer code using the above model to predict the particle behavior in the VC chamber were performed. $k - \varepsilon$ model was employed for the calculation of the gas flow field. This section presents some of the typical results with regard to the distributions of gas and particle velocities and gas/particle slip velocities.

## 3.1 Calculation basis

### Boundary and initial conditions

The predictions were made on the bench-scale VC model which serves as the boundary conditions. Detailed description of the bench-scale model can be found in the previous reports [1, 5]. The major dimensions of the model are listed in Table 4. The inlet conditions of gas and particle flows at the nozzle exit are summarized in Table 5.

$k - \varepsilon$ turbulence model was used to correlate the Reynolds stress for the computation of gas flow field. Particles were calculated in Lagrangian framework by the newly developed

Table 4 Major dimensions of the bench-scale VC model

| | |
|---|---|
| Chamber diameter (I.D.) | 10" |
| Chamber height | 26" |
| Center pipe diameter (O.D.) | 5" |
| Center pipe length | 20" - 12" (adjustable) |
| Interval between | |
| primary air and lower sec. air nozzle sets | 2.2" |
| lower sec. air and middle sec. air nozzle sets | 7.2" |
| middle sec. air and upper sec. air nozzle sets | 7.4" |

Table 5 Inlet conditions of gas and particle flows

| | | |
|---|---|---|
| Gas flow rate | 57 | $m^3$ /hr |
| Nozzle exit velocity | 9 | m/s |
| Particle | | |
| tangential velocity | 6 | m/s |
| radial velocity | 1.2 | m/s |
| axial velocity | 2.4 | m/s |

statistical-trajectory model. 1,000 particles were calculated and the results are presented in the following paragraph.

## 3.2 Numerical Results

The axial velocity distributions of gas and particle flows are depicted in Fig. 14. Significant changes of the velocity profile along the height of the vortex chamber can be observed. It is seen that the particle velocity profile may not necessarily follow that of the gas. Fig. 15 gives the particle tangential velocity distributions. It is interesting to note that the

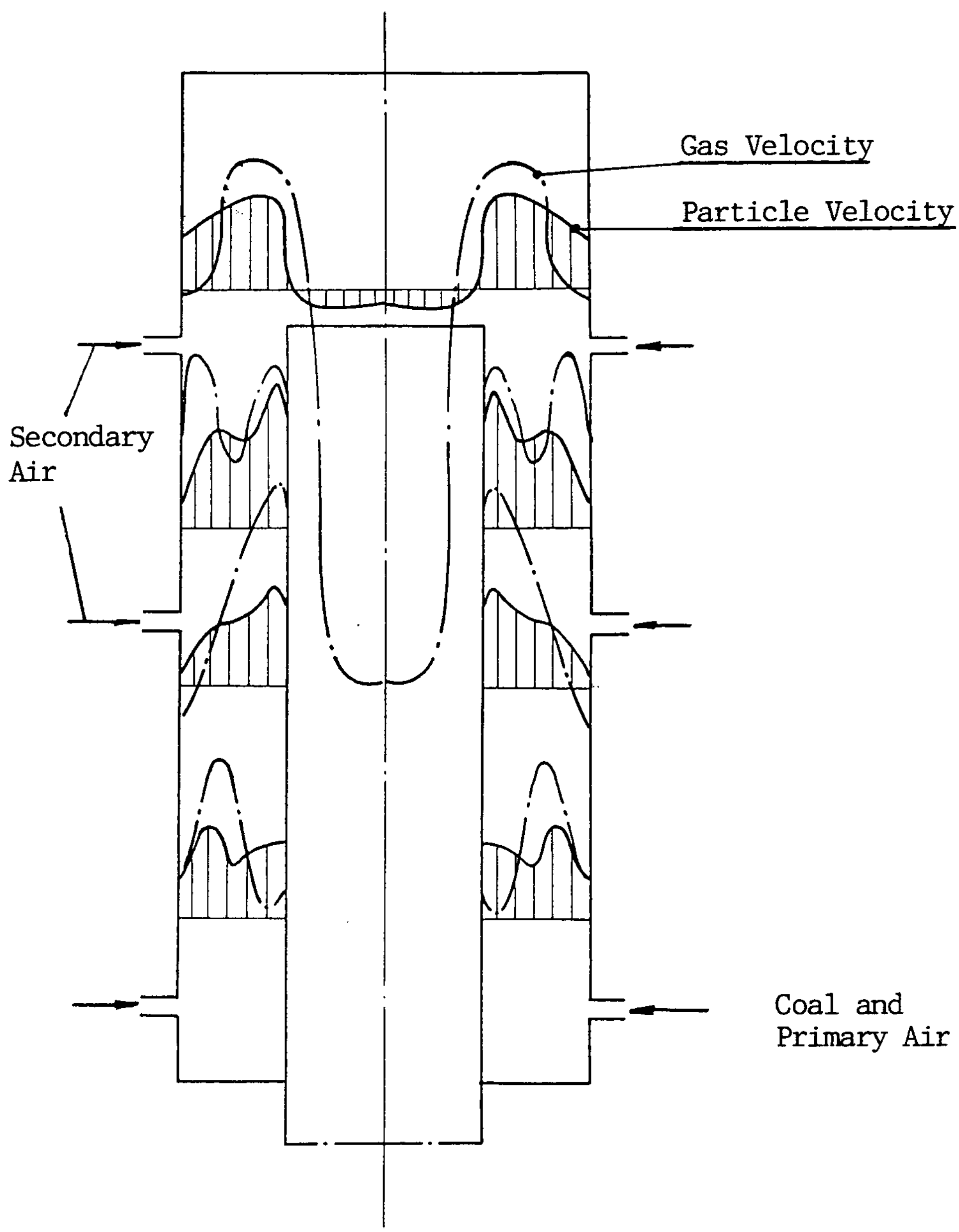


Fig. 14 Axial Velocity Distributions of Gas and Particle Flows

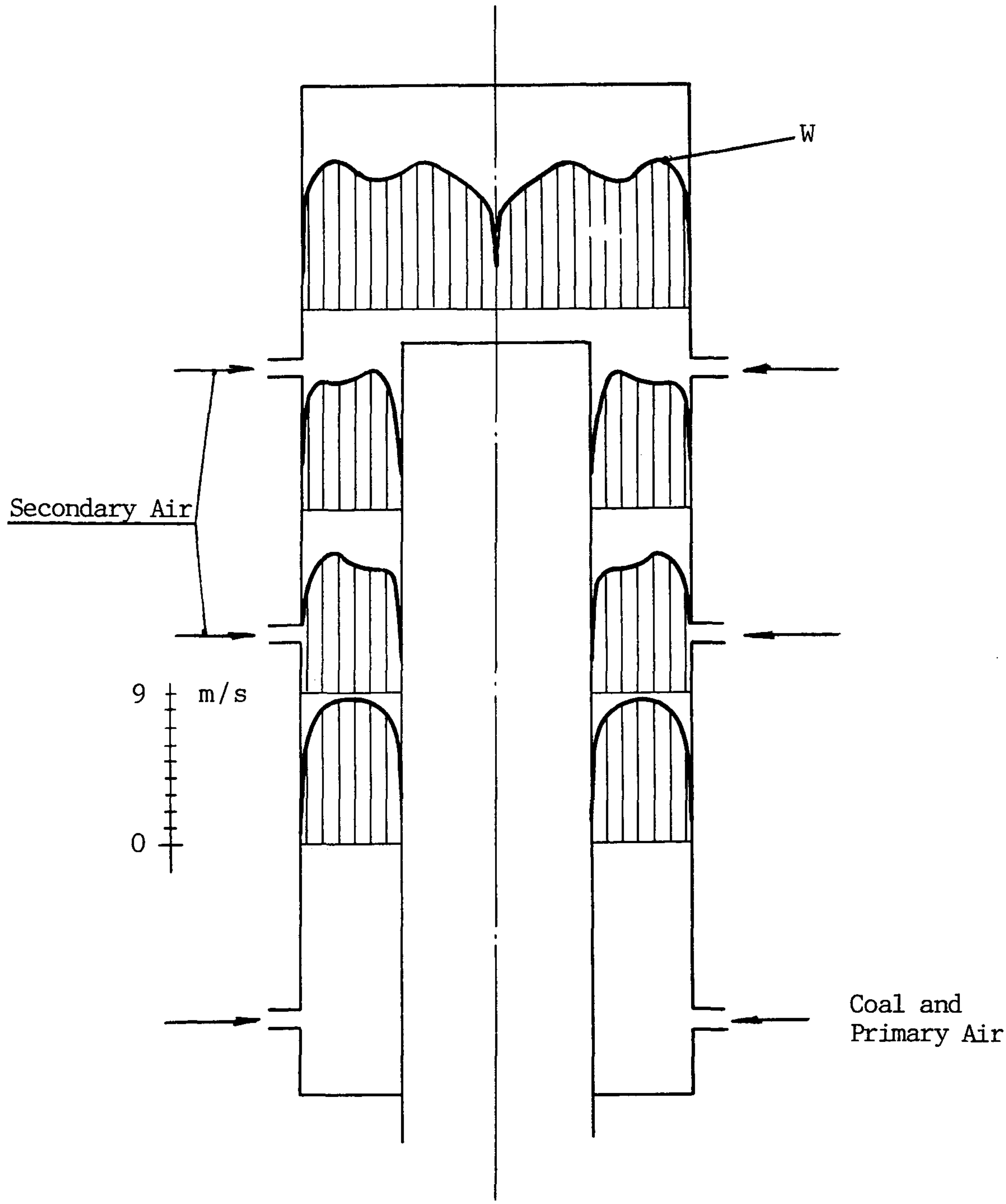


Fig. 15 Distribution of Particle Tangential Velocity

distributions of particle tangential velocities are smooth in both the annular space and the cylindrical volume above the center pipe top. However, measurement results of the aerodynamics showed that the gas tangential velocity distributions change significantly in this cylindrical volume. This implies that high gas-particle slip velocity could be achieved in the VC chamber, especially in the cylindrical volume. This was verified by the computational results as shown in Figure 16. It is seen that large gas-particle slip velocities exist in almost the entire VC chamber with the maximum values in the cylindrical zone. The large gas-particle slip velocity in the VC chamber is deemed highly favorable for the initiation of fuel ignition and burn-off of char residue. To increase the slip velocity is essential to the burn-off of char residue in small particles. Experimental and numerical results have shown that small particles have relatively short residence time due to the small particle terminal velocity. Therefore, in order to have those particles burnt completely during their short stay in the VC chamber, to increase the reaction rate seems to be an effective option. Hence, the large gas-particle slip velocity, which enhances phase mixing and heat and mass transfer between the gas phase and particle phases, can be utilized to effectively increase the carbon conversion efficiency of the vortex combustor.

Parametric studies regarding dynamic control of particle behavior and the interaction between the gas and particle phases will be the future efforts in the VC mathematical modeling work.

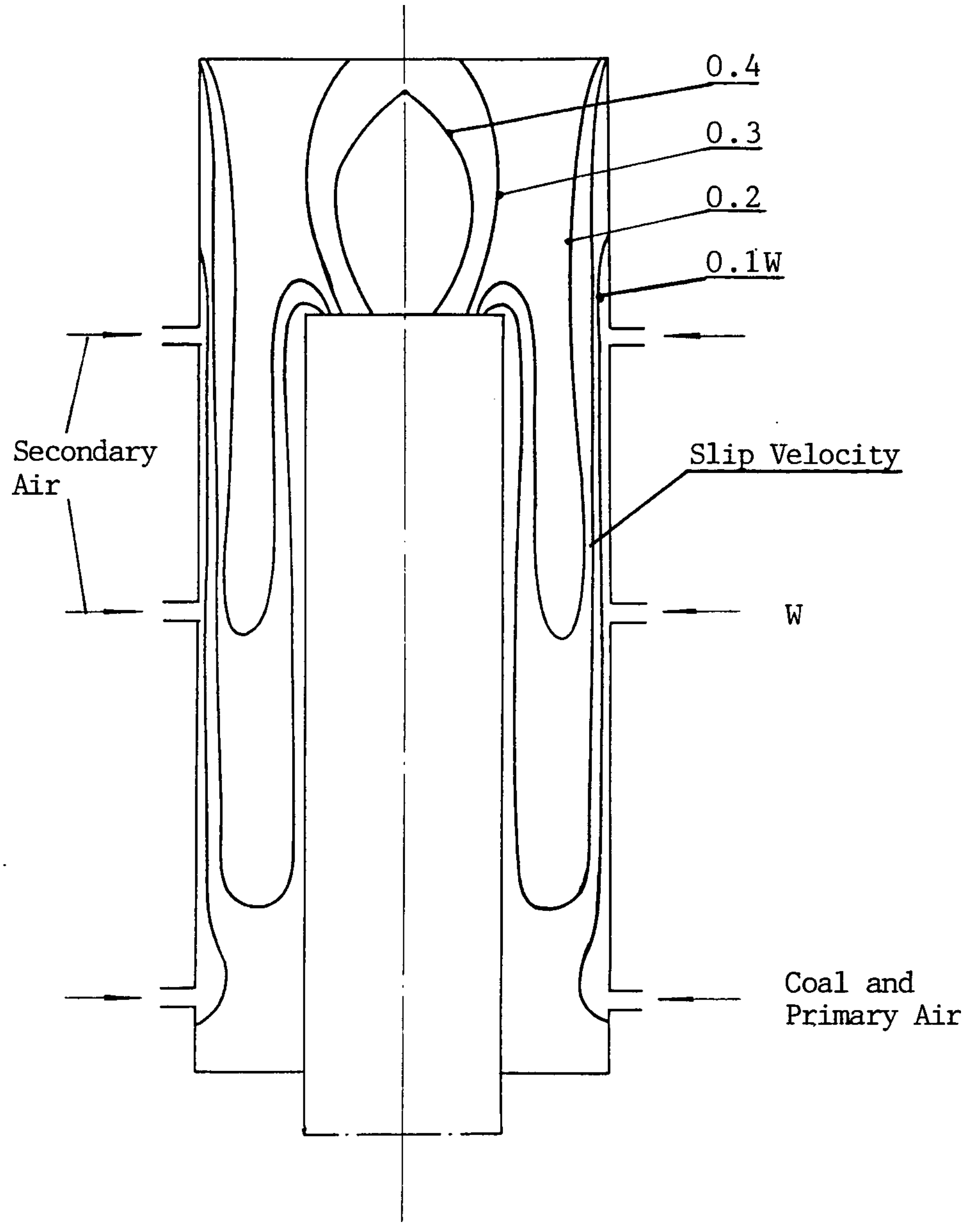


Fig. 16 Distributions of Gas-Particle Slip Velocities

## REFERENCES


[1] Nieh, S., "Development of a Vortexing Combustor (VC) for Space/Water Heating Applications (Cold Flow Modeling)", Technical Progress Report No. 3 for PRDA No. DE-AC22-87PC79661 to Pittsburgh Energy Technology Center, U.S. DOE, February, 1988.

[2] Nieh, S., "Development of a Vortexing Combustor (VC) for Space/Water Heating Applications (Cold Flow Modeling)", Technical Progress Report No. 4 for PRDA No. DE-AC22-87PC79661 to Pittsburgh Energy Technology Center, U.S. DOE, May, 1988.

[3] Nieh, S., "Exploratory Vortex Combustor (VC) Development", Report to Naval Civil Engineering Laboratory, under contract No. N62583/88 M X756, June, 1988.

[4] Zhao, C., "Swirl Number in VC Combustors", internal research progress report to Prof. S. Nieh, Department of Mechanical Engineering, The Catholic University of America, August, 1988.

[5] Nieh, S., "Development of a Vortexing Combustor (VC) for Space/Water Heating Applications (Cold Flow Modeling)", Technical Progress Report No. 2 for PRDA No. DE-AC22-87PC79661 to Pittsburgh Energy Technology Center, U.S. DOE, November, 1987.